Title

Characterization of Growth, Glomerular Number, and Tubular Proteins in the Developing Rhesus Monkey Kidney

Permalink

https://escholarship.org/uc/item/39w3r9nh

Journal

The Anatomical Record, 296(11)

ISSN

1932-8486

Authors

Batchelder, Cynthia A
Keyser, Jennifer L
Lee, C Chang I
et al.

Publication Date

2013-11-01

DOI

10.1002/ar.22756

Peer reviewed

Characterization of Growth, Glomerular Number, and Tubular Proteins in the Developing Rhesus Monkey Kidney

Cynthia A. Batchelder[1], **Jennifer L. Keyser**[1], **C. Chang I. Lee**[1], and **Alice F. Tarantal**[1,2,*]

[1]California National Primate Research Center, School of Medicine, University of California, Davis, California

[2]Departments of Pediatrics and Cell Biology and Human Anatomy, School of Medicine, University of California, Davis, California

Abstract

An essential step in the translation of cell-based therapies for kidney repair involves preclinical studies in relevant animal models. Regenerative therapies in children with congenital kidney disease may provide benefit, but limited quantitative data on normal development is available to aid in identifying efficient protocols for repair. Nonhuman primates share many developmental similarities with humans and provide an important translational model for understanding nephrogenesis and morphological changes across gestation. These studies assessed monkey kidney size and weight during development and utilized stereological methods to quantitate total number of glomeruli. Immunohistochemical methods were included to identify patterns of expression of tubular proteins including Aquaporin-1 (AQP1), AQP2, Calbindin, E-Cadherin, and Uromodulin. Results have shown that glomerular number increased linearly with kidney weight, from 1.1×10^3 in the late first trimester to 3.5×10^5 near term ($P < 0.001$). The ratio of glomeruli to body weight tripled from the late first to early second trimester then remained relatively unchanged. Only AQP1 was expressed in the proximal tubule and descending Loop of Henle. The ascending Loop of Henle was positive for AQP2, Calbindin, and Uromodulin; distal convoluted tubules stained for Calbindin only; and collecting tubules expressed AQP2 and E-Cadherin with occasional Calbindin-positive cells. These findings provide quantitative information on normal kidney ontogeny in rhesus monkeys and further support the importance of this model for human kidney development.

Keywords

kidney; nephrogenesis; monkey; stereology; fetus

Disruption of normal kidney development is a major cause of renal disease and accounts for nearly one-third of all childhood kidney-related illnesses (NIH, 2000). While animal models have elucidated important molecular and cellular events associated with congenital obstructive nephropathy and renal dysplasia (Chevalier et al., 2010), underlying causes

*Correspondence to: Alice F. Tarantal, Ph.D., California National Primate Research Center, 1 Shields Avenue, University of California, Davis, Davis, CA 95616-8542. Fax: +530–752-2880. aftarantal@primate.ucdavis.edu.

remain largely unknown, and few long-term therapeutic options are available. Of the pediatric patients undergoing kidney dialysis in 2011, 26.8% resulted from renal dysplasia or obstructive renal disease (NAPRTCS, 2011), and the number of pediatric patients with end-stage renal disease due to congenital kidney abnormalities has increased nearly 12% in the last 10 years (US Renal Data System, 2010). Although dialysis and kidney transplantation provides short-term solutions for children with kidney disease, the development of cellular therapies holds promise for longer term treatments.

Animal models are crucial to explore regenerative strategies for all age groups, and these models require a detailed understanding of kidney development in order to effectively identify potential new methods for kidney repair. Rhesus monkeys are an important translational model as this species has a close phylogenetic relationship and similar kidney ontogeny when compared with humans (Lee et al., 2001; Tarantal et al., 2001; Matsell and Tarantal, 2002; Batchelder et al., 2009, 2010; Leapley et al., 2009). The fetal rhesus monkey model of obstructive renal dysplasia recapitulates the molecular and cellular pathology observed in humans and provides a unique and essential model for studies of regenerative therapies (Tarantal et al., 2001, 2012; Matsell et al., 2002). In addition to studies of pathogenesis (Tarantal et al., 2001; Matsell et al., 2002; Butt et al., 2007; Hiatt et al., 2010) key studies with the monkey model include the evaluation of the temporal and spatial expression of key renal developmental markers (Batchelder et al., 2010), new methods to differentiate human embryonic stem cells toward renal precursors (Batchelder et al., 2009), the growth and culture of renal cortical cells (Leapley et al., 2009), the assessment of methods to radiolabel and image *in vivo* transplanted renal precursors (Tarantal et al., 2012), and the development of natural kidney scaffolds for renal tissue engineering (Nakayama et al., 2010, 2011). A unique challenge in the development of engineered constructs is the need to consider basic organization of tissue (morphology, protein expression) in an age-related and functional context. Future advances in this field are dependent on a thorough knowledge of the developmental morphology of the kidney in the chosen model species, quantitative parameters for assessment, and establishment of functional markers that can be used to analyze cells or tissue engineered constructs. In this study, stereology and immunohistochemistry were used to further characterize normal renal ontogeny in the rhesus monkey, and to establish baseline parameters of kidney growth, glomerular content, and the onset of tubular functional protein expression including Aquaporin-1 (AQP1), a proximal tubule water channel; Uromodulin, an ascending Loop of Henle marker also known as Tamm-Horsfall glycoprotein; AQP2, a collecting duct water channel; Calbindin, a calcium binding protein; as well as E-cadherin, a distal tubule and collecting duct cell adhesion protein.

Materials and Methods

Animals

All animal procedures were performed according to the requirements of the Animal Welfare Act and protocols were approved before implementation by the Institutional Animal Care and Use Committee at the University of California, Davis. Adult female rhesus monkeys (*Macaca mulatta*) with a history of prior pregnancies (N = 23) were bred and identified as

pregnant using established sonographic methods (Tarantal, 2005). Length of gestation in the rhesus monkey is 165 ± 10 days (Tarantal and Gargosky, 1995), with pregnancy divided into trimesters by 55-day increments (0–55 days = first trimester, 56–110 days = second trimester, 111–165 days = third trimester). Primate Center standard operating procedures were followed for all activities related to animal care including diet and housing. Fetal growth was monitored by ultrasound during gestation and findings compared to normative growth charts (Tarantal, 2005). Tissues were collected following hysterotomy during the first trimester (50 ± 2 days gestation), second trimester (80 ± 2 and 100 ± 2 days gestation), and third trimester (120 ± 2 and 150 ± 2 days gestation) using established methods (Tarantal et al., 2001). Kidneys from postnatal animals (3 months, N = 3) were also collected according to standard protocols for immunohistochemical comparison (Nakayama et al., 2010). Measurements collected at the time of tissue harvest included body weight, kidney weight, and kidney length and width (Table 1).

Tissue Processing and Sectioning

Kidneys were collected and measured then placed in 4% paraformaldehyde immediately postcollection for 4 hr at 4°C, then embedded in 4% Agar (Fisher Scientific, Waltham, MA) in appropriately sized round isector molds using a custom design (Fig. 1). The round isector molds were then embedded in rectangular molds in paraffin to ensure isotropic uniform random orientation (Nyengaard and Gundersen, 1992). Paraffin blocks were exhaustively sectioned at 5–8 μm and a minimum of 10 sets of serial sections were collected to guarantee adequate point counts for reproducible and accurate data collection. To ensure uniform sampling, a random start was selected for the first set of serial sections collected, and then all following sets of serial sections were selected at fixed intervals to guarantee consistent thickness between sampled sections. In this manner, 10–15 groups of 25 serial sections were collected at consistent intervals across the kidneys. Sections were also stained with hematoxylin and eosin (H&E) using standard protocols, and assessed by unbiased stereological methods. An estimate of the total number of glomeruli was also obtained by the stereological fractionator-physical disector approach of Pakkenberg and Gundersen (1988). Briefly, the number of glomeruli was determined by the product of the glomerular count and the reciprocal of the sampling fraction at each fractionation step.

Stereology

Selected sections were scanned using an Olympus VS110 Virtual Microscopy System to create digital images at 1×, 10×, and 40× magnification. The Computer Assisted Stereological Toolbox (C.A.S.T.) software (Olympus America, Melville, NY) was used to apply point-counting grids or to select and align reference and look-up frames to assist with unbiased counting. The Cavalieri method was used to estimate total kidney and cortical volumes (Gundersen and Jensen, 1987). Briefly, a point grid at 1× magnification was used to obtain a count of all grid points overlying the cortex and the kidney for estimation of total volumes. The reference volume was estimated from the product of the thickness (distance from one counted section to the next), the area/point in the counting grid, and the sum of all points overlying the area of interest (cortex). Unbiased counting frames were applied to serial sections obtained by a physical disector (Pakkenberg and Gundersen, 1988) to estimate the numerical density of glomeruli in the cortex. Glomeruli present in the look-up

frame, but not the reference frame, were marked and counted (Sterio, 1984). The directional counting rule of the physical disector was applied to increase efficiency of the procedure by enabling reversal of the look-up and reference frames for an additional count (Howard and Reed, 2005). Multiplication of the numerical density of glomeruli in the cortex by the volume of the cortex provided an estimate of the total number of glomeruli.

Histology and Immunohistochemistry

Sections were prepared for immunohistochemical staining by deparaffinization followed by rehydration in graded ethanol according to established protocols (Lee et al., 2001; Tarantal et al., 2001; Batchelder et al., 2009). Heat-induced antigen retrieval was accomplished with 0.01 M citrate buffer (pH 6.0, Life Technologies, Grand Island, NY). Primary antibodies used included AQP1 (clone H-55, 1:500 dilution, Santa Cruz Biotechnology, Santa Cruz, CA), AQP2 (clone C-17, 1:100 dilution, Santa Cruz Biotechnology), Uromodulin (polyclonal, 1:100 dilution, Sigma-Aldrich, St Louis, MO), Calbindin (clone D_{28K}, 1:100, EMD Millipore, Billerica, MA), and E-Cadherin (clone NCH-38, 1:100, Dako, Glostrup, Denmark). Slides were mounted with ProLong Gold antifade reagent with 4′6-diamidino-2-phenylindole (DAPI) (Life Technologies) before coverslip placement.

Statistical Analysis

Results are presented as mean ± standard error of the mean (SEM). Paired *t* tests and analysis of variance were used to determine statistical significance ($P < 0.05$).

Results

Morphology

Stereologic and morphologic methods were utilized to quantitate kidney development in the rhesus monkey as a basis for studies of cellular regeneration and tissue engineering. All tissues were evaluated morphologically by H&E staining, with no abnormalities confirmed. Representative photomicrographs of the developing kidney in the late first trimester (50 ± 2 days gestation), early second trimester (80 ± 2 days gestation), late second trimester (100 ± 2 days gestation), early third trimester (120 ± 2 days gestation), and near term (150 ± 2 days gestation) are shown in Fig. 1. Mean kidney weights, lengths, and widths are shown in Table 1. Fetal weight increased nearly 100-fold from the late first trimester (5.27 ± 1.01 g) to the third trimester (505.25 ± 26.11 g) while individual kidney weight increased more than 200-fold (0.02 ± 0.01 g vs. 1.58 ± 0.13 g). No significant differences between the measures and weights of the right and left kidneys were detected (data not shown). The ratio of individual kidney weight to fetal body weight increased from the late first trimester (2.86 ± 0.82) to a maximum in the second trimester (4.01 ± 0.07) ($P < 0.0005$) with a decrease at term (3.11 ± 0.20).

Stereology

Fetal kidneys were collected utilizing an isotropic approach in order to preserve precious tissues in such a manner as to allow stereological analysis of various structures including glomeruli and tubules. The Cavalieri method (to estimate total kidney and cortex volume) and the physical disector approach (to estimate glomerular density) were combined to

estimate total number of glomeruli (Fig. 2A). Exhaustive sectioning and tabulation of counted sections provided a means to compare the isector counting approach with the 'gold standard' stereological approach (physical disector-fractionator) (Pakkenberg and Gundersen, 1988) for counting the number of homogeneous structures. The estimated number of glomeruli per kidney across gestation was similar and highly correlated (correlation coefficient = 0.99) between both stereological approaches. The number of glomeruli per kidney increased more than 28-fold from the late first trimester (1.1×10^3) to the early second trimester (3.2×10^4) ($P < 0.001$), then increased 24.1fold by the early third trimester (1.3×10^5) ($P < 0.01$). In the third trimester, the number of glomeruli increased an additional 2.5-fold with an estimate of 3.5×10^5 glomeruli per kidney near term. From the first trimester to the early second trimester, the mean number of glomeruli per gram fetal body weight increased nearly three-fold suggesting rapid formation of glomeruli (Fig. 2B). In contrast, the number of glomeruli relative to fetal body weight was relatively unchanged for the remainder of gestation (mean 1.1×10^3 glomeruli/g fetal body weight). A linear trend ($R^2 = 0.90$) was observed between the number of glomeruli and kidney weight indicating a proportional increase in the number of glomeruli with kidney growth (Fig. 2C).

Immunohistochemistry

In order to assess the temporal and spatial expression patterns of key tubule proteins across ontogeny, immunohistochemistry was performed. The proximal tubule water channel AQP1 was not observed in the nephrogenic zone but was expressed in some, but not all, developing tubules in the late first trimester (Fig. 3). From the second trimester onward, AQP1 was observed in the proximal convoluted tubules, proximal straight tubules, and descending Loop of Henle. The ureteric bud and surrounding condensed mesenchyme were noted with dim expression of the vasopressin-responsive water channel AQP2 in the late first trimester (Fig. 4). Beginning in the second trimester, bright AQP2 expression was noted in structures consistent with the ascending Loop of Henle and the collecting ducts. Some cells of the parietal epithelium of Bowman's capsule expressed AQP2 by the late third trimester. Calbindin, a calcium binding protein, was strongly expressed in the central ureteric bud stalks but diminished where bud tips were surrounded by condensed mesenchyme from the late first trimester through the early second trimester (Fig. 5). By the late second trimester, Calbindin expression was noted in all cells of the distal convoluted tubules and some, but not all, cells of the collecting ducts, and this finding continued throughout the third trimester.

For positive identification of the ascending Loop of Henle, dual staining of AQP2 with the Tamm-Horsfall glycoprotein marker Uromodulin was performed (Fig. 6). Some developing tubule-like structures were positive for both markers in the late first trimester. In the second trimester and thereafter, only structures consistent with ascending Loop of Henle morphology expressed both AQP2 and Uromodulin. Dual staining of Calbindin with the epithelial marker, E-Cadherin, or with AQP2 was assessed for further identification of developing renal tubular structures. The ureteric bud expressed Calbindin and E-Cadherin but not AQP2. Of the markers tested, only AQP1 was expressed in proximal tubules and the descending Loop of Henle (Fig. 3). The ascending Loop of Henle was positive for AQP2 (Fig. 4), Calbindin (Fig. 5), and Uromodulin (Fig. 6) with distal convoluted tubules staining

for Calbindin only (Fig. 6), and collecting tubules expressing E-Cadherin (Fig. 6) and AQP2 (Fig. 4) with occasional Calbindin-positive cells (Fig. 6). The parietal epithelium of Bowman's capsule modestly expressed AQP1 and AQP2.

Discussion

Development of the definitive fetal kidney (metanephros) is a highly orchestrated process between the ureteric bud and the metanephric blastema involving reciprocal interactions as the branching ureteric epithelium induces differentiation of the metanephric mesenchyme which, in turn, stimulates further branching of the ureteric epithelium (Saxen, 1987). As kidney development proceeds, the induced mesenchyme forms renal vesicles with further differentiation leading to comma-and S-shaped bodies. Additional steps in glomerular and tubular differentiation results in formation of various tubular segments of the mature nephron and specialized glomerular cell populations. While these morphological events have been described and the role of specific markers such as Pax2 (Dressler and Douglass, 1992) and WT1 (Pritchard-Jones et al., 1990) identified, quantitative data for objective assessment of normal kidney ontogeny remains limited. Our studies have previously shown that kidney development in the rhesus monkey follows a pattern similar to human kidney development with active nephrogenesis evident from the late first through mid-third trimester (Batchelder et al., 2010). The data presented here establish additional quantitative standards for normal kidney development in this species, further support the value of this model for studies focused on human renal disease, and provides a useful baseline for future studies to address repair.

Stereological methods provide a reliable, precise, and efficient method for quantifying kidney structures (Nyengaard, 1999; Bertram, 2001; Cullen-McEwen et al., 2012a,b). Although the sectioning process is extensive, counting of structures and calculations of volumes, surface areas, and lengths can be efficiently performed when stereological methods are used, and without assumptions that may not be valid regarding the shape of structures such as glomeruli. To apply these methods correctly, considerable effort must be directed to ensure unbiased random sampling in three dimensions and to minimize the influence of technical issues such as those that may occur from tissue shrinkage during the preservation or sectioning processes (Bertram et al., 2000). The use of the isector molds in these studies assured unbiased random sampling, an essential component for estimation of parameters such as volume and length (e.g., tubules), with no assumptions regarding size, shape, or location of the glomeruli. The number of glomeruli estimated with the isector approach was remarkably similar to the number of glomeruli estimated by the physical disector-fractionator approach that is considered the stereological 'gold-standard'. These studies establish the validity of the isector counting approach utilized especially when samples are precious and additional analyses requiring the isector method may be desired. These techniques permit accurate quantification of morphological changes and the evaluation of relationships between structures with organ and whole body weight.

Studies of fetal kidney development utilizing stereological methods in animal models include rats (Bertram et al., 2000; Cullen-McEwen et al., 2011), sheep (Bains, 1996), and baboons (Gubhaju et al., 2009). Estimation of glomerular number in adult African green

monkeys has been reported to be 1.27×10^5 (Skov et al., 1999) and 1.13×10^5 (Skov et al., 2001) glomeruli per kidney; juxtamedullary glomeruli were noted to increase in volume when compared with cortical glomeruli. The number of glomeruli estimated in adult African green monkeys was approximately three-fold less than the number of glomeruli estimated in fetal rhesus monkeys in this study, which likely reflects differences in age groups. Others have reported a decline in the number of glomeruli with age in adult humans (Nyengaard and Bendtsen, 1992; Rule et al., 2010; Hoy et al., 2011). It is important to note that rodents complete nephrogenesis postnatally, which differs when compared to human and nonhuman primates where nephrogenesis is completed before birth. The number of glomeruli present at the end of nephrogenesis in normal rats (Bertram et al., 1992; Cullen-McEwen et al., 2011) and mice (Basgen et al., 2006; David et al., 2010) are considerably less than reported in large animal models such as pigs (Lødrup et al., 2008), sheep (Wintour et al., 2003), baboons (Gubhaju et al., 2009), humans (Nyengaard and Bendtsen, 1992; Hoy et al., 2003; Keller et al., 2003; White et al., 2007; McNamara et al., 2010), and monkeys as shown in Skov et al. (1999, 2001) and in the studies described herein (see Table 2).

The developing rhesus monkey kidney was further characterized through immunohistochemical assessment of expression patterns of several proteins crucial to the water balance function of the kidney. A majority of absorption of water from the glomerular filtrate occurs via osmosis through the water channel AQP1 (Agre et al., 1993) located in proximal tubule epithelium in rodents and humans (Maunsbach et al., 1997; Bedford et al., 2003), and localized similarly in monkeys as shown in these studies. While AQP1 is essential for passive water reabsorption in the proximal nephron, AQP2 is the vasopressin-responsive water channel in the distal nephron responsible for tight control of plasma volume and an essential protein for concentration of urine (Christensen et al., 2003; Rojek et al., 2006). Previous studies localized AQP2 to connecting tubules and collecting duct cells in mice (Nelson et al., 1998), rats (Fushimi et al., 1993; Nielsen et al., 1993), and humans (Sasaki et al., 1994), a pattern also confirmed in rhesus monkeys. Expression of these key proteins in the fetal kidney was previously noted to differ in humans when compared with rodents, as AQP1 and AQP2 were not evident until the mid-third trimester in these species (Yamamoto et al., 1997) but were observed as early as the late first trimester in humans (Devuyst et al., 1996) and rhesus monkeys as noted. Other studies have reported a unique and potential regenerative role for cells of the parietal epithelium (Ronconi et al., 2009) which, in these studies, were found to stain with tubular markers AQP1 and AQP2 in the late third trimester, suggesting further exploration of the role of the parietal epithelial cells in tubular repair is warranted.

Potential therapies for congenital obstructive renal disease will likely involve repair with tissue-engineered constructs (Nakayama et al., 2010, 2011, 2013). When applied prenatally (Tarantal et al., 2012) such strategies may effectively allow for organ growth and development in synchronization with the growing patient, and further underscores the importance of animal models that can best simulate human development. The normative range of values established for the temporal and spatial appearance of renal functional markers in the fetal and infant kidney provides important benchmarks by which to assess disease models, cellular therapeutics, and regenerative strategies for repair.

In summary, results of this study establish quantitative parameters of kidney growth, glomerular content, and the onset of tubular functional proteins in rhesus monkeys, and further establish similarities with human kidney development. These studies provide important information for enhancing our understanding of kidney ontogeny and the crucial developmental milestones for future translational studies focused on organ repair in the monkey model of obstructive renal disease.

Acknowledgments

Literature Cited

Agre P, Preston GM, Smith BL, Jung JS, Raina S, Moon C, Guggino WB, Nielsen S. Aquaporin CHIP: the archetypal molecular water channel. Am J Physiol. 1993; 265:463–476.

Bains RK, Sibbons PD, Murray RD, Howard CV, Van Velzen D. Stereological estimation of the absolute number of glomeruli in the kidneys of lambs. Res Vet Sci. 1996; 60:122–125. [PubMed: 8685532]

Basgen JM, Nicholas SB, Mauer M, Rozen S, Nyengaard JR. Comparison of methods for counting cells in the mouse glomerulus. Nephron Exp Nephrol. 2006; 103:139–148.

Batchelder CA, Lee CCI, Matsell DG, Yoder MC, Tarantal AF. Renal ontogeny in the rhesus monkey (*Macaca mulatta*) and directed differentiation of human embryonic stem cells towards kidney precursors. Differentiation. 2009; 78:45–56. [PubMed: 19500897]

Batchelder CA, Lee CCI, Martinez ML, Tarantal AF. Ontogeny of the kidney and renal developmental markers in the rhesus monkey (*Macaca mulatta*). Anat Rec. 2010; 293:1971–1983.

Bedford JJ, Leader JP, Walker RJ. Aquaporin expression in normal human kidney and in renal disease. J Am Soc Nephrol. 2003; 14:2581–2587. [PubMed: 14514735]

Bertram JF, Soosaipillai MC, Ricardo SD, Ryan GB. Total numbers of glomeruli and individual glomerular cell types in the normal rat kidney. Cell Tissue Res. 1992; 270:37–45. [PubMed: 1423523]

Bertram JF, Young RJ, Spencer K, Gordon I. Quantitative analysis of the developing rat kidney: absolute and relative volumes and growth curves. Anat Rec. 2000; 258:128–135. [PubMed: 10645960]

Bertram JF. Counting in the kidney. Kidney Int. 2001; 59:792–796. [PubMed: 11168963]

Butt MJ, Tarantal AF, Jimenez DF, Matsell DG. Collecting duct epithelial-mesenchymal transition in fetal urinary tract obstruction. Kidney Int. 2007; 72:936–944. [PubMed: 17667982]

Chevalier RL, Thornhill BA, Forbes MS, Kiley SC. Mechanisms of renal injury and progression of renal disease in congenital obstructive nephropathy. Pediatr Nephrol. 2010; 25:687–697. [PubMed: 19844747]

Christensen BM, Wang W, Frokiaer J, Nielsen S. Axial heterogeneity in basolateral AQP2 localization in rat kidney: effect of vasopressin. Am J Physiol Renal Physiol. 2003; 284:701–717.

Cullen-McEwen LA, Armitage JA, Nyengaard JR, Moritz KM, Bertram JF. A design-based method for estimating glomerular number in the developing kidney. Am J Physiol Renal Physiol. 2011; 300:1448–1453.

Cullen-McEwen LA, Armitage JA, Nyengaard JR, Bertram JF. Estimating nephron number in the developing kidney using the physical disector/fractionator combination. Methods Mol Biol. 2012a; 886:109–119. [PubMed: 22639255]

Cullen-McEwen LA, Douglas-Denton RN, Bertram JF. Estimating total nephron number in the adult kidney using the physical disector/fractionator combination. Methods Mol Biol. 2012b; 886:333–350. [PubMed: 22639275]

David FS, Cullen-McEwen L, Wu XS, Zins SR, Lin J, Bertram JF, Neel BG. Regulation of kidney development by Shp2: an unbiased stereological analysis. Anat Rec. 2010; 293:2147–2153.

Devuyst O, Burrow CR, Smith BL, Agre P, Knepper MA, Wilson PD. Expression of aquaporins-1 and -2 during nephrogenesis and in autosomal dominant polycystic kidney disease. Am J Physiol. 1996; 271:169–183.

Dressler GR, Douglass EC. Pax-2 is a DNA-binding protein expressed in embryonic kidney and Wilms' tumor. Proc Natl Acad Sci USA. 1992; 89:1179–1183. [PubMed: 1311084]

Fushimi K, Uchida S, Hara Y, Hirata Y, Marumo F, Sasaki S. Cloning and expression of apical membrane water channel of rat kidney collecting tubule. Nature. 1993; 361:549–552. [PubMed: 8429910]

Gubhaju L, Sutherland MR, Yoder BA, Zulli A, Bertram JF, Black MJ. Is nephrogenesis affected by preterm birth? Studies in a non-human primate model. Am J Renal Physiol. 2009; 297:1668–1677.

Gundersen HJG, Jensen EG. The efficiency of systematic sampling in stereology and its prediction. J Microsc. 1987; 147:229–263. [PubMed: 3430576]

Hiatt MJ, Ivanova L, Toran N, Tarantal AF, Matsell DG. Remodeling of the fetal collecting duct epithelium. Am J Pathol. 2010; 176:630–637. [PubMed: 20035053]

Howard, CV.; Reed, MG. Unbiased Stereology. 2nd. New York, NY: Garland Science/BIOS Scientific Publishers; 2005.

Hoy WE, Douglas-Denton RN, Hughson MD, Cass A, Johnson K, Bertram JF. A stereological study of glomerular number and volume: preliminary findings in a multiracial study of kidneys at autopsy. Kidney Int. 2003; 63:S31–S37.

Hoy WE, Hughson MD, Diouf B, Zimanyi M, Samuel T, McNamara BJ, Douglas-Denton RN, Holden L, Mott SA, Bertram JF. Distribution of volumes of individual glomeruli in kidneys at autopsy: association with physical and clinical characteristics and with ethnic group. Am J Nephrol. 2011; 33:15–20. [PubMed: 21659730]

Keller G, Zimmer G, Mall G, Ritz E, Amann K. Nephron number in patients with primary hypertension. N Engl J Med. 2003; 348:101–108. [PubMed: 12519920]

Leapley AC, Lee CCI, Batchelder CA, Yoder MC, Matsell DG, Tarantal AF. Characterization and culture of fetal rhesus monkey renal cortical cells. Pediatr Res. 2009; 66:448–454. [PubMed: 19581826]

Lee CI, Goldstein O, Han VK, Tarantal AF. IGF-II and IGF binding protein (IGFBP-1, IGFBP-3) gene expression in fetal rhesus monkey tissues during the second and third trimesters. Pediatr Res. 2001; 49:379–387. [PubMed: 11228264]

Lødrup AB, Karstoft K, Dissing TH, Pedersen M, Nyengaard JR. Kidney biopsies can be used for estimations of glomerular number and volume: a pig study. Virchows Arch. 2008; 452:393–403. [PubMed: 18214535]

Matsell DG, Mok A, Tarantal AF. Altered primate glomerular development due to *in utero* urinary tract obstruction. Kidney Int. 2002; 61:1263–1269. [PubMed: 11918732]

Matsell DG, Tarantal AF. Experimental models of fetal obstructive nephropathy. Pediatr Nephrol. 2002; 27:470–476. [PubMed: 12172756]

Maunsbach AB, Marples D, Chin E, Ning G, Bondy C, Agre P, Nielsen S. Aquaporin-1 water channel expression in human kidney. J Am Soc Nephrol. 1997; 8:1–14. [PubMed: 9013443]

McNamara BJ, Diouf B, Douglas-Denton RN, Hughson MD, Hoy WE, Bertram JF. A comparison of nephron number, glomerular volume and kidney weight in Senegalese Africans and African Americans. Nephrol Dial Transplant. 2010; 25:1514–1520. [PubMed: 20154008]

Mitchell EK, Louey S, Cock ML, Harding R, Black MJ. Nephron endowment and filtration surface area in the kidney after growth restriction of fetal sheep. Pediatr Res. 2004; 55:769–773. [PubMed: 14973179]

Nakayama KH, Batchelder CA, Lee CI, Tarantal AF. Decellularized rhesus monkey kidney as a three-dimensional scaffold for renal tissue engineering. Tissue Eng Part A. 2010; 16:2207–2210. [PubMed: 20156112]

Nakayama KH, Batchelder CA, Lee CI, Tarantal AF. Renal tissue engineering with decellularized rhesus monkey kidneys: age-related differences. Tissue Eng Part A. 2011; 17:2891–2901. [PubMed: 21902603]

Nakayama KH, Lee CCI, Batchelder CA, Tarantal AF. Tissue specificity of decellularized rhesus monkey kidney and lung scaffolds. PLoS One. 2013; 8:e64134. [PubMed: 23717553]

National Institutes of Health, NIDDK, ASPN. Pediatric Nephrology Task Force Publication; 2000. Research Needs in Pediatric Kidney Disease: 2000 and Beyond. Available online at http://www2.niddk.nih.gov/NR/rdonlyres/DC7B952F-9CDD-44DD-B0ABBFE79A774AE5/0/Pediatric_Kidney_Disease_2000_and_-Beyond.pdf [Last accessed 3/1/13]

Nelson RD, Stricklett P, Gustafson C, Stevens A, Ausiello D, Brown D, Kohan DE. Expression of an AQP2 cre recombinase transgene in kidney and male reproductive system of transgenic mice. Am J Physiol. 1998; 275:216–226.

Nielsen S, DiGiovanni SR, Christensen EI, Knepper MA, Harris HW. Cellular and subcellular immunolocalization of vasopressin-regulated water channel in rat kidney. Proc Natl Acad Sci USA. 1993; 90:11663–11667. [PubMed: 8265605]

North American Pediatric Renal Trials and Collaborative Studies (NAPRTCS). Annual Dialysis Report 2011. The EMMES Corporation; Rockville, MD: 2011.

Nyengaard JR. Stereologic methods and their application in kidney research. J Am Soc Nephrol. 1999; 10:1100–1123. [PubMed: 10232698]

Nyengaard JR, Bendtsen TF. Glomerular number and size in relation to age, kidney weight, and body surface in normal man. Anat Rec. 1992; 232:194–201. [PubMed: 1546799]

Nyengaard JR, Gundersen HJG. The isector: a simple and direct method for generating isotropic, uniform random sections from small specimens. J Microsc. 1992; 165:427–431.

Pakkenberg B, Gundersen HJ. Total number of neurons and glial cells in human brain nuclei estimated by the disector and the fractionator. J Microsc. 1988; 150:1–20. [PubMed: 3043005]

Pritchard-Jones K, Fleming S, Davidson D, Bickmore W, Porteous D, Gosden C, Bard J, Buckler A, Pelletier J, Housman D, van Heyningen V, Hastie N. The candidate Wilm's tumour gene is involved in genitourinary development. Nature. 1990; 346:194–197. [PubMed: 2164159]

Rojek A, Fuchtbauer EM, Kwon TH, Frokiaer J, Nielsen S. Severe urinary concentrating defect in renal collecting duct-selective AQP2 conditional-knockout mice. Proc Natl Acad Sci USA. 2006; 103:6037–6042. [PubMed: 16581908]

Ronconi E, Sagrinati C, Angelotti ML, Lazzeri E, Mazzinghi B, Ballerini L, Parente E, Becherucci F, Gacci M, Carini M, Maggi E, Serio M, Vannelli GB, Lasagni L, Romagnani S, Romagnani P. Regeneration of glomerular podocytes by human renal progenitors. J Am Soc Nephrol. 2009; 20:322–332. [PubMed: 19092120]

Rule AD, Amer H, Cornell LD, Taler SJ, Coslo FG, Kremers WK, Textor SC, Stegall MD. The association between age and nephrosclerosis on renal biopsy among healthy adults. Ann Intern Med. 2010; 152:561–567. [PubMed: 20439574]

Sasaki S, Fushimi K, Saito H, Saito F, Uchida S, Ishibashi K, Kuwahara M, Ikeuchi T, Invi K, Nakajima K, Watanabe TX, Marumo F. Cloning, characterization, and chromosomal mapping of human aquaporin of collecting duct. J Clin Invest. 1994; 93:1250–1256. [PubMed: 7510718]

Saxen, L. Organogenesis of the kidney. In: Barlow, PW.; Green, PB.; White, CC., editors. Developmental and Cell Biology Series. Vol. 19. Cambridge, UK: Cambridge University Press; 1987. p. 1-171.

Skov K, Nyengaard JR, Patwardan A, Mulvany MJ. Large juxtamedullary glomeruli and afferent arterioles in healthy primates. Kidney Int. 1999; 55:1462–1469. [PubMed: 10201011]

Skov K, Hamet P, Nyengaard JR, Mulvany MJ. Morphology of renal afferent arterioles and glomeruli, heart weight, and blood pressure in primates. Am J Hypertens. 2001; 14:331–337. [PubMed: 11336178]

Sterio DC. The unbiased estimation of number and sizes of arbitrary particles using the disector. J Microsc. 1984; 134:127–136. [PubMed: 6737468]

Tarantal, AF. Ultrasound imaging in rhesus (*Macaca mulatta*) and long-tailed (*Macaca fascicularis*) macaques: reproductive and research applications. In: Woolfe-Coote, S., editor. The Laboratory Primate. Amsterdam: Elsevier; 2005. p. 317-351.

Tarantal AF, Gargosky SE. Characterization of the insulin-like growth factor (IGF) axis in the serum of maternal and fetal macaques (*Macaca mulatta* and *Macaca fascicularis*). Growth Regul. 1995; 5:190–198. [PubMed: 8745144]

Tarantal AF, Han VK, Cochrum KC, Mok A, daSilva M, Matsell DG. Fetal rhesus monkey model of obstructive renal dysplasia. Kidney Int. 2001; 59:446–456. [PubMed: 11168926]

Tarantal AF, Lee CC, Batchelder CA, Christensen JE, Prater D, Cherry SR. Radiolabeling and *in vivo* imaging of transplanted renal cell lineages differentiated from human embryonic stem cells in fetal rhesus monkeys. Mol Imaging Biol. 2012; 14:197–204. [PubMed: 21479709]

U.S. Renal Data System. USRDS 2010 Annual Data Report: Atlas of Chronic Kidney Disease and End-Stage Renal Disease in the United States. National Institutes of Health, National Institute of Diabetes and Digestive and Kidney Diseases; Bethesda, MD: 2010.

White KE, Marshall SM, Bilous RW. Are glomerular volume differences between type 1 and type 2 diabetic patients pathologically significant? Diabetologia. 2007; 50:906–912. [PubMed: 17333103]

Wintour EM, Moritz KM, Johnson K, Ricardo S, Samuel CS, Dodic M. Reduced nephron number in adult sheep, hypertensive as a result of prenatal glucocorticoid treatment. J Physiol. 2003; 549:929–935. [PubMed: 12730337]

Yamamoto T, Sasaki S, Fushimi K, Ishibashi K, Yaoita E, Kawaski K, Fujinaka H, Marumo F, Kihara I. Expression of AQP family in rat kidneys during development and maturation. Am J Physiol Renal Physiol. 1997; 272:198–204.
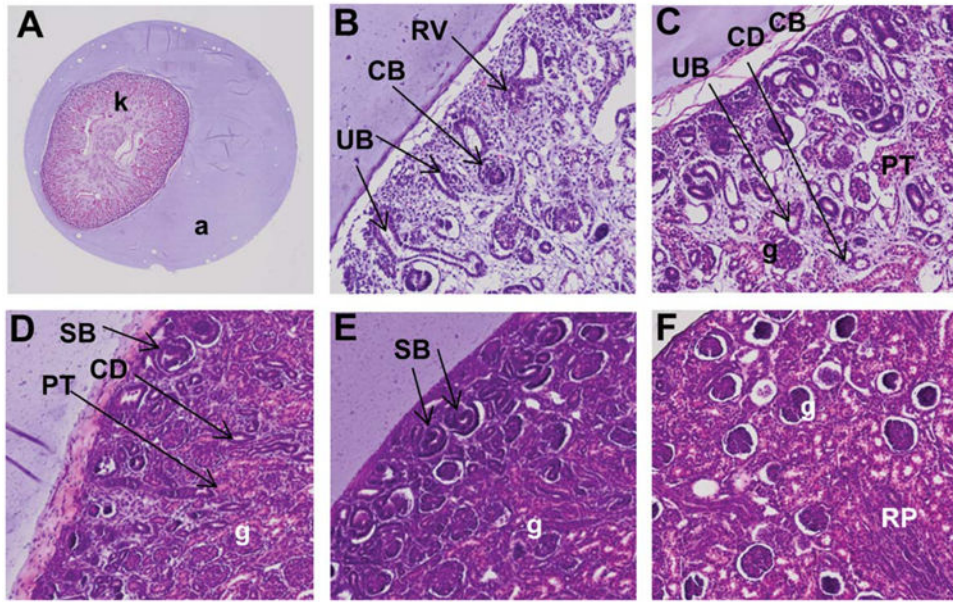
Fig. 1.
Kidney development in fetal rhesus monkeys. (**A**) Kidneys (k) were embedded in a round isector mold in agar (a) followed by re-embedding in rectangular paraffin molds to ensure isotropic random orientation. Representative photomicrographs of developing monkey kidneys in the late first trimester (**B**), early (**C**) and late (**D**) second trimester, and early (**E**) and late (**F**) third trimester. Images (10×) stained with H&E are oriented with the cortex to the upper left and the medulla to the lower right. CD, collecting duct; CB, comma or C-shaped body; g, glomerulus; PT, proximal tubule; RP, renal papilla; RV, renal vesicle; SB, S-shaped body; UB, ureteric bud.
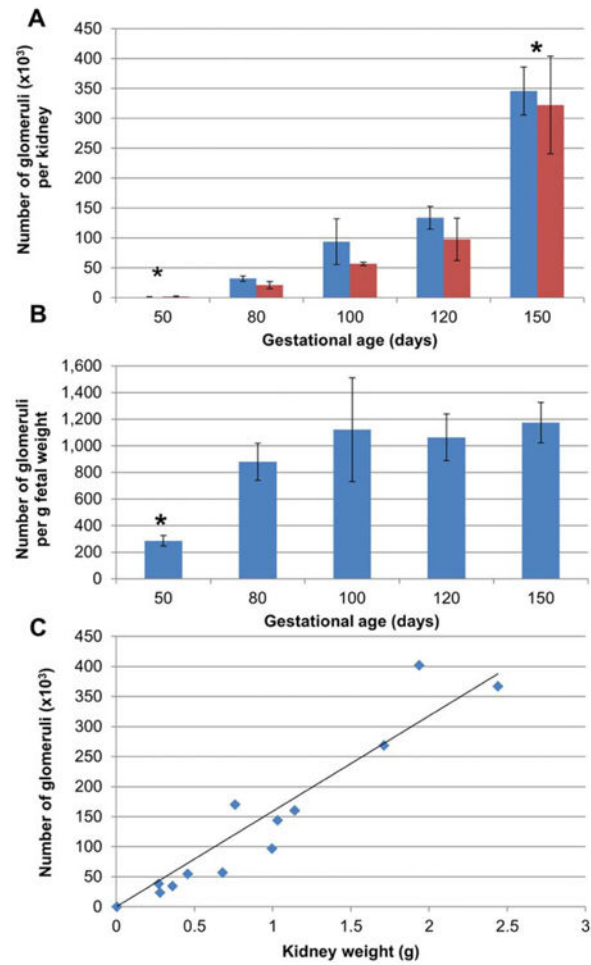
Fig. 2.
Relationship between glomerular number, kidney weight, body weight, and gestational age.
(**A**) Glomerular counts were determined by two stereological methods: isector (blue bars)
and physical disector/fractionator (red bars) with no significant differences noted between
methods. The number of glomeruli per kidney increased with advancing gestational age (*P
< 0.001). (**B**) The number of glomeruli per gram of kidney remained unchanged across the
second and third trimesters. (**C**) A linear relationship was shown between the number of
glomeruli and kidney weight.
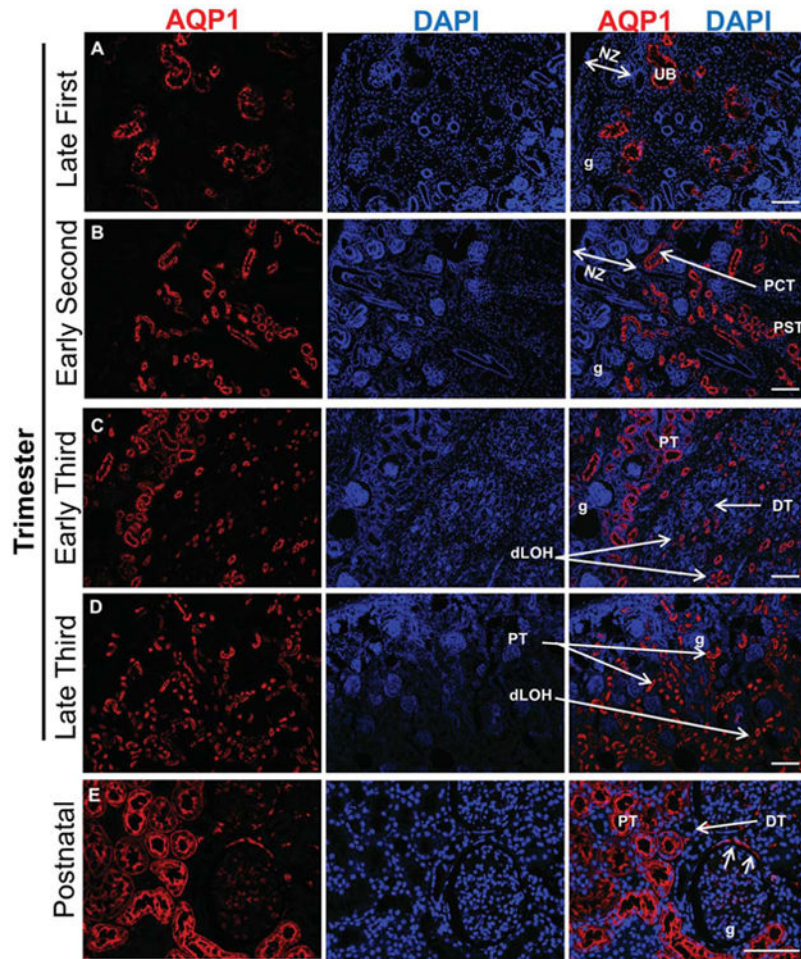
Fig. 3.
Aquaporin-1 (AQP1) expression in developing monkey kidneys. (**A**) AQP1 was not observed in the nephrogenic zone (NZ) but was expressed in some, but not all, developing tubules in late first trimester. (**B–D**) From the second trimester onward, AQP1 was observed in structures within the proximal convoluted tubule (PCT), proximal straight tubule (PST), descending Loop of Henle (dLOH), and occasionally in some cells of the parietal epithelium of Bowman's capsule (arrows). DT, distal tubule; g, glomerulus; PT, proximal tubule; UB, ureteric bud. Scale bar= 100 μm.
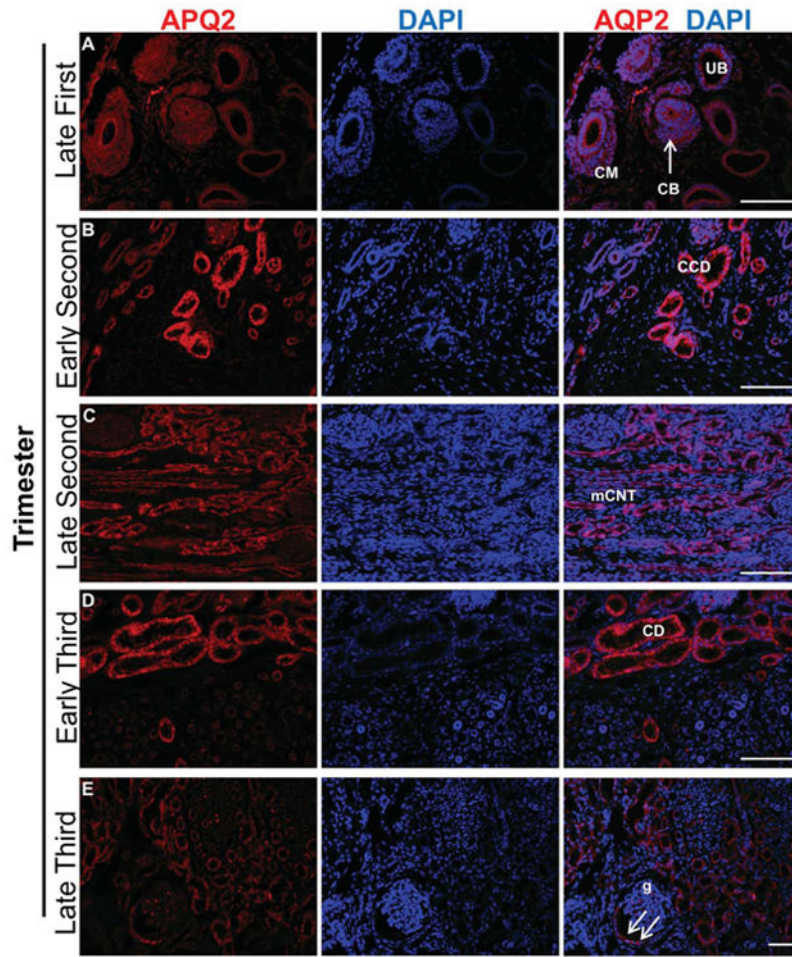
Fig. 4.
AQP2 expression in developing monkey kidneys. (**A**) Ureteric bud (UB) and surrounding condensed mesenchyme (CM) were noted with dim expression in the late first trimester. (**B–D**) Beginning early in the second trimester, bright AQP2 expression was noted in structures consistent with the ascending Loop of Henle and the collecting ducts (CD). (**E**) Some cells of the parietal epithelium of Bowman's capsule expressed AQP2 by the late third trimester (arrows). CB, C-shaped body; CCD, cortical collecting duct; g, glomerulus; mCNT, medullary connecting tubule. Scale bar =100 μm.
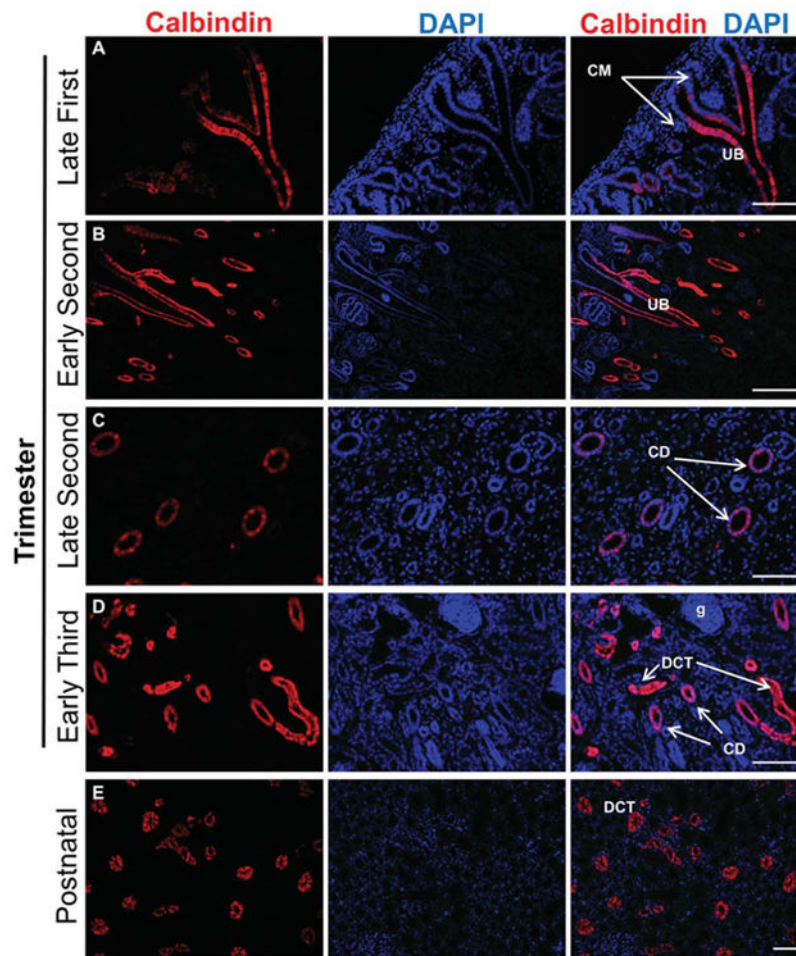
Fig. 5.
Calbindin expression in developing monkey kidneys. (**A** and **B**) Expression was observed in central ureteric bud (UB) stalks but reduced where bud tips were surrounded by condensed mesenchyme (CM). (**C** and **D**) In the late second trimester, expression was noted in all cells of the distal convoluted tubules (DCT) and some, but not all, cells of the collecting ducts (CD). g, glomerulus. Scale bar = 100 μm.
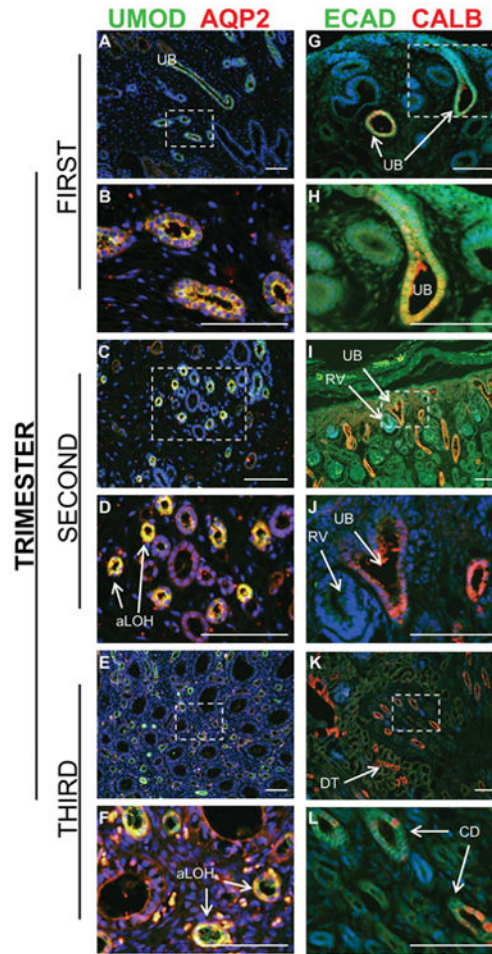
Fig. 6.
Expression of Uromodulin (UMOD), AQP2, Calbindin, and E-Cadherin in developing monkey kidneys. Boxes denoted with dashed lines in upper images (**A, C, E, G, I, K**) represent areas magnified in lower image (**B, D, F, H, J, L**). Nuclei visualized with DAPI (blue). (**A** and **B**) Some developing tubule structures were positive for both UMOD and AQP2 in the late first trimester. (**C–F**) In the second trimester and thereafter, only the ascending LOH (aLOH) expressed both AQP2 and UMOD. (**G–J**) The ureteric bud (UB) expressed Calbindin (CALB) and E-Cadherin (ECAD) with a loss of expression in the differentiating bud tips and renal vesicles (RV). (**K–L**) CALB was expressed in distal tubules (DT) and coexpressed with ECAD in some cells of the collecting ducts (CD) in the medullary rays. Scale bar = 100 μm.

Table 1

Overview of fetal measurements (mean ± SEM)

Gestational age (days)	50 ± 2 (First trimester)	80 ± 2 (Second trimester)	100 ± 2 (Second trimester)	120 ± 2 (Third trimester)	150 ± 2 (Third trimester)
Kidney weight (g)	0.02 ± 0.01	0.20 ± 0.07	0.68 ± 0.05	0.86 ± 0.08	1.58 ± 0.13
Kidney length (mm)	2.80 ± 0.30	11.23 ± 0.62	14.47 ± 0.35	15.03 ± 1.20	19.58 ± 0.52
Kidney width (mm)	2.17 ± 0.29	8.10 ± 0.48	10.11 ± 0.16	11.74 ± 0.73	12.86 ± 0.31
Body weight (BW) (g)	5.27 ± 1.01	73.86 ± 5.89	168.42 ± 12.27	252.00 ± 14.42	505.25 ± 26.11
Kidney weight/BW ratio[a]	2.86 ± 0.82	2.93 ± 1.11	4.01 ± 0.07	3.44 ± 0.34	3.11 ± 0.20

[a] Calculated for individual animals before determining the mean ± SEM.

Table 2

Comparison between species and age group for glomerular number and kidney to body weight (BW) ratio

Species	Age group	# Glomeruli/kidney	Kidney weight/BW ratio
Rat[a]	Term	0.5×10^4	–
Sheep[b,c]	Term	$3.0–5.6 \times 10^5$	2.8
Monkey	Term	3.4×10^5	3.1
Baboon[d]	Midthird trimester	0.3×10^6	3.9
Pig[e]	Juvenile	2.1×10^6	–
Mouse[f,g]	Adult	1.2×10^4	–
Rat[a,h]	Adult	3.2×10^4	–
Sheep[i]	Adult	4.0×10^5	1.2
Monkey[j,k]	Adult	$1.1–1.3 \times 10^5$	1.8–2.0
Human[l-p]	Adult	$0.6–1.4 \times 10^6$	2.0–2.2

[a]Cullen-McEwen et al. (2011).

[b]Bains et al. (1996).

[c]Mitchell et al. (2004).

[d]Gubhaju et al. (2009).

[e]Lødrup et al. (2008).

[f]Basgen et al. (2006).

[g]David et al. (2010).

[h]Bertram et al. (1992).

[i]Wintour et al. (2003).

[j]Skov et al. (1999).

[k]Skov et al. (2001).

[l]Nyengaard and Bendtsen (1992).

[m]Hoy et al. (2003).

[n]Keller et al. (2003).

[o]White et al. (2007).

[p]McNamara et al. (2010).